

Particle-in-cell and Monte Carlo simulation of the hydrogen plasma immersion ion implantation process

Dixon Tat-Kun Kwok and Paul K. Chu^{a)}

Department of Physics & Materials Science, City University of Hong Kong, 83 Tat Chee Avenue, Kowloon, Hong Kong

Blake P. Wood

Los Alamos National Laboratory, PO Box 1663, MSE526, Los Alamos, New Mexico 87545

Chung Chan

Department of Electrical and Computer Engineering, Northeastern University, Boston, Massachusetts 02115

(Received 27 January 1999; accepted for publication 5 May 1999)

Hydrogen plasma immersion ion implantation into a 200-mm-diam silicon wafer placed on top of a cylindrical stage has been numerically simulated by the particle-in-cell (PIC) and transport-and-mixing-from-ion-irradiation (TAMIX) methods. The PIC simulation is conducted based on the plasma comprising three hydrogen species H^+ , H_2^+ , and H_3^+ in a ratio determined by secondary ion mass spectrometry. The local sputtering losses and retained doses are calculated by the Monte Carlo code TAMIX. The combined effect of the three species results in a maximum retained dose variation of 11.6% along the radial direction of the wafer, although the implanted dose variation derived by PIC is higher at 21.5%. Our results suggest that the retained dose variations due to off-normal incident ions can partially compensate for variations in incident dose dictated by plasma sheath conditions. The depth profile becomes shallower toward the edge of the wafer. Our results indicate that it is about 34% shallower at the edge, but within a radius of 6.375 cm, the depth of the peak only varies by about 5%. For plasma implantation process design, a combination of PIC and TAMIX is better than the traditional practice of using PIC alone. © 1999 American Institute of Physics. [S0021-8979(99)02716-4]

I. INTRODUCTION

Plasma immersion ion implantation (PIII) has created a great deal of interest in semiconductor processing due to its high dose rate and simple instrumentation.¹⁻⁴ In PIII, a target such as a silicon wafer is immersed in a plasma and a high negative potential relative to the chamber wall usually in a pulsed mode is applied to the sample. Electrons are repelled away while ions in the plasma are accelerated across the sheath formed around the target and implanted into the surface of the wafer. Under low-pressure conditions the sheath thickness has to be smaller than the mean free path of the ions for the sheath to be collisionless. In addition, since the entire wafer is implanted simultaneously, the implantation time is independent of wafer size, and this time advantage over conventional beam-line ion implantation is greater for a larger wafer size, such as 300 mm. PIII has been utilized to form shallow junctions,⁵⁻⁸ synthesize silicon-on-insulator (SOI) structures,⁹⁻¹⁷ and process flat panel display materials.¹⁸

SOI is the preferred material over bulk silicon substrates for high speed, low voltage complementary metal oxide semiconductor (CMOS) integrated circuits.¹⁹ A bond-cut process, commercially referred to as Smart-Cut™ developed by SOITEC, has been successful in producing SOI wafers.^{20,21} One of the critical steps of Smart-Cut™ is to

implant a fairly high dose of hydrogen or helium into the wafer to form a plane along which the wafer can cleave. After implantation, the wafer is bathed in a high-pH solution and hydrophilically bonded with an oxide-coated substrate at low temperature. The bonded wafer cracks along the implanted hydrogen peak region by annealing at 500 °C, and the SOI structure is finally annealed at 1100 °C for 60 min to solidify the bonding.¹² For partially depleted CMOS devices, the implantation energy is typically high in order to implant hydrogen deep into the wafer to form thick SOI wafers. On the other hand, for fully depleted CMOS devices requiring thinner SOI, conventional beam-line ion implantation can be substituted by PIII to accomplish a higher throughput and lower cost. In order to design the appropriate PIII conditions, it is customary to perform theoretical simulation to narrow down the process window before experiments are conducted. The simulation formalisms commonly used by plasma scientists and process engineers are the fluid model or particle-in-cell (PIC) model.²²⁻²⁵ These two methods, however, only impart information pertaining to the plasma, but fail to take into account solid state interaction like sputtering or predict practical parameters such as retained doses in the silicon wafer.

In order for PIII to compete with conventional beam-line ion implantation as a commercial technique, the thickness uniformity of the SOI wafers prepared by the PIII/ion-cut process must be similar to that attained by conventional beam-line ion implantation. Recently, we have discovered

^{a)} Author to whom correspondence should be addressed; electronic mail: paul.chu@cityu.edu.hk

that the sample stage (chuck) design can impact ion uniformity significantly, and a plane wafer holder with no quartz covers yields the most uniform ion dose distribution across the wafer.^{26,27} We have also identified that ions impact the wafer at various angles and energies by experiments and using PIC simulation.²⁸ In this work, we combine PIC with the Monte Carlo code TAMIX to investigate the relationship between the incident dose and the retained dose, the latter being more important to process engineers. Hydrogen PIII into a plane wafer is numerically simulated by the PIC method based on the plasma being composed of three hydrogen ion species H^+ , H_2^+ , and H_3^+ in a ratio determined experimentally by secondary ion mass spectroscopy (SIMS). The retained doses, depth profiles, and surface recessions along the radial distance of the wafer stage are calculated by TAMIX, a Monte Carlo ion implantation code developed at the University of Wisconsin, Madison.²⁹ Our results show that the maximum difference in the retained dose along the radial direction on the silicon wafer is 11.6%, and the implant depth profile is fairly uniform within the inner circle of radius 2/3 of the wafer. The combined use of PIC and TAMIX thus presents a closer picture of reality than PIC alone.

II. PIII SIMULATION PROCESS

We use a kinetic model to describe the motion of ions and the details have been described elsewhere.²⁶ Under low-pressure hydrogen PIII conditions, the ions are assumed to be noncollisional and cold, and they acquire directed motion by the electric field. The electrons are in thermal equilibrium and the electron density is given by Boltzmann's relation:

$$n_e = n_0 \exp\left(\frac{e\phi}{kT_e}\right), \quad (1)$$

where n_0 is the initial total ion density, k is the Boltzmann's constant, T_e is the electron temperature, and e is the electron charge. Poisson's equation relates the potential ϕ to the electron density n_e and total ion density n_i . The plasma consists of three singularly charged hydrogen species, H^+ , H_2^+ , and H_3^+ , in different proportion. Poisson's equation is rewritten as:

$$\nabla^2 \phi = -\frac{e}{\epsilon_0} [n_i(H^+ + n_i(H_2^+) + n_i(H_3^+) - n_e)], \quad (2)$$

where ϵ_0 is the permittivity in free space. The motions of the ions are governed by Newton's equations of motion.²⁶ The force acting on the three hydrogen species are the same, since they are singularly charged:

$$\mathbf{F} = -q\nabla\phi. \quad (3)$$

However, they have different masses and their acceleration will be different from each other. Consequently, their density distributions will be different, in turn affecting the total ion density and expansion of the sheath. Although noncollisional conditions are satisfied in low pressure PIII, we should not carry out separate simulation for each species and obtain the resultant dose by adding the individual doses together. Instead, we have to carry out simulation combining their ef-

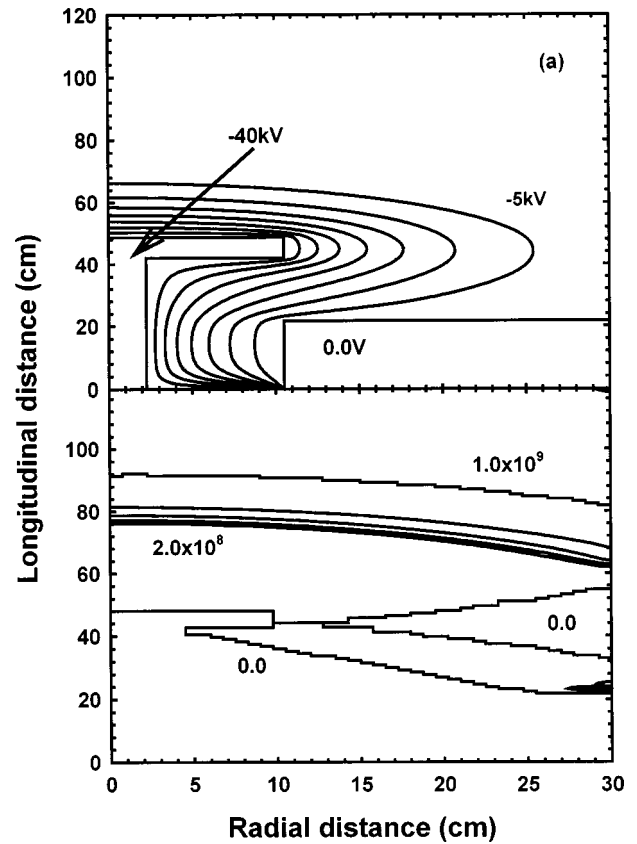


FIG. 1. (a) Potential contour lines and (b) combined ion density contour lines at $15 \mu s$. Contour intervals are -5 kV and 2.0×10^8 , respectively.

fects employing Eq. (2). The equations are expressed in cylindrical coordinates and the plasma quantities are made dimensionless by normalization.²⁶ The simulation parameters are not only based on the dimension of the PIII instrument in the City University of Hong Kong, but also on the specific geometry of that particular instrument.^{1,17} The height of the cylindrical vacuum chamber is 100.0 cm and radius is 33.75 cm. The wafer stage is supported by a stainless steel rod of radius 2.25 cm extending from a well recessed below the vacuum chamber. The depth of the well is 22.5 cm and radius is 11.25 cm. The total length of the rod is 42.5 cm and the wafer stage is elevated by 20.0 cm from the bottom of the chamber. The wafer stage platen is 6.75 cm thick and 10.50 cm in radius. We apply 40 kV to the wafer stage, and the electron temperature is assumed to be 4.0 eV. The total ion density of the hydrogen plasma is $1 \times 10^9 \text{ cm}^{-3}$ which is typical for the hydrogen PIII/ion-cut process. The ratio $H^+ : H_2^+ : H_3^+$ is 0.05 : 0.317 : 0.633 as determined experimentally by SIMS yielding H^+ , H_2^+ , and H_3^+ densities of 5.0×10^7 , 3.17×10^8 , and $6.33 \times 10^8 \text{ cm}^{-3}$, respectively. It takes $2.0 \mu s$ for the applied voltage to linearly rise to -40 kV and each implantation pulse stops after $15.0 \mu s$.

III. RESULTS AND DISCUSSION

The potential and combined ion density contour lines at $15.0 \mu s$ are displayed in Fig. 1. The dynamic sheath touches the chamber walls and expands upwards. The ions are drawn

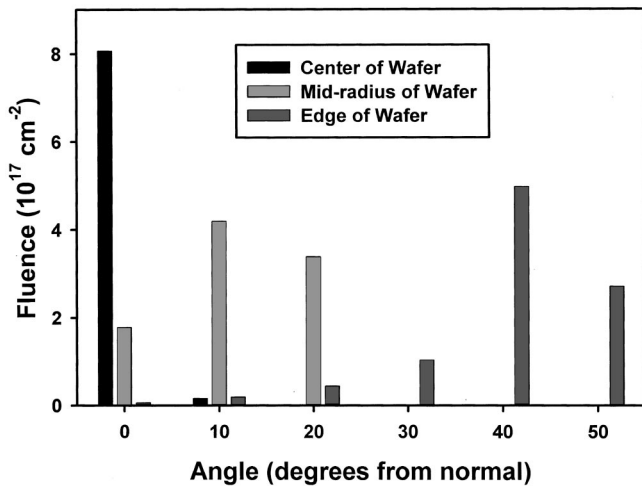


FIG. 2. Angular distribution from normal of the accumulated implanted ion dose (fluence given in number of atoms) for all three species at the center of the wafer, in the middle of the wafer (radius between 5.25 and 6.0 cm), and at the wafer edge (radius between 9.75 and 10.0 cm).

away from the chamber wall starting from the plane parallel to the wafer stage. We divide the wafer into 14 equal boxes of 0.75 cm in width from the center to the edge. The fluence and impact energy distribution against the impact angle of each box are recorded for a single pulse. We observe that ions impact normally around the center area but the impact angle is more oblique at the edge. The angular distributions from normal of the accumulated implanted ion doses and impact energy at the center, midway, and edge of the wafer are depicted in Fig. 2. It shows that the three hydrogen species are implanted at an angle between 40° and 50° from normal near the wafer edge, while most ions are implanted

perpendicularly into the wafer center. There is no significant difference among individual species, since they are subjected to the same accelerating field.

The angular distribution information of each box is subsequently input into TAMIX to calculate the surface profile. To imitate the realistic conditions, the target is implanted with 5.929×10^6 pulses, so that the total H atom incident dose from all three species at the location with the highest fluence is $1.0 \times 10^{18} \text{ cm}^{-2}$. Note that an H_3^+ ion contributes three H atoms, although at an implant energy of 13.3 keV rather than 40 keV, similarly for H_2^+ at 20 keV per hydrogen atom. To compare the combined and separate effect of the three hydrogen species, we carry out four TAMIX runs: H^+ , H_2^+ , and H_3^+ individually and one with all three species together. TAMIX can take a maximum of ten combinations of energy angle. We have to throw out the lowest fluence combinations when there are more than ten. For instance, for outside positions, there are typically five angles for each species, so there are $3 \times 5 = 15$ total energy-angle combinations for the combined run, and five of these must be discarded. We do not believe that this makes much difference in the results, since the ones thrown out typically contribute only a few percent of the peak fluence.

The fluences and retained doses (hydrogen atoms) along the radial distance of the four different runs are shown in Fig. 3. The fluence stemming from H^+ is 50 times less than the total fluence, since the plasma contains predominantly H_2^+ and H_3^+ ions. It is thus obvious that the influence of the H_3^+ ion will dominate the hydrogen atom distribution profile since the plasma contains 63.3% of H_3^+ ions and it counts as three hydrogen atoms. The ratio of the retained to incident doses for the three hydrogen species is different. It is observed that it is highest for H^+ as depicted in Fig. 3(a) and only about half of the incident H_3^+ is retained as shown in

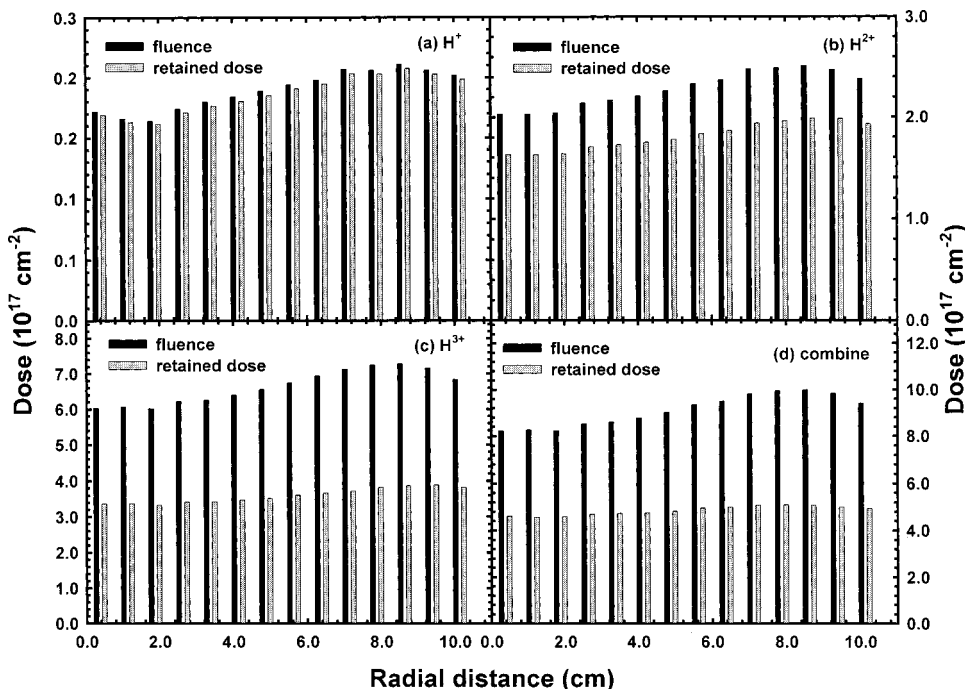


FIG. 3. Fluence and retained dose (hydrogen atoms) along the radial distance of (a) H^+ , (b) H_2^+ , (c) H_3^+ , and (d) the three species together. The retained doses are calculated by TAMIX.

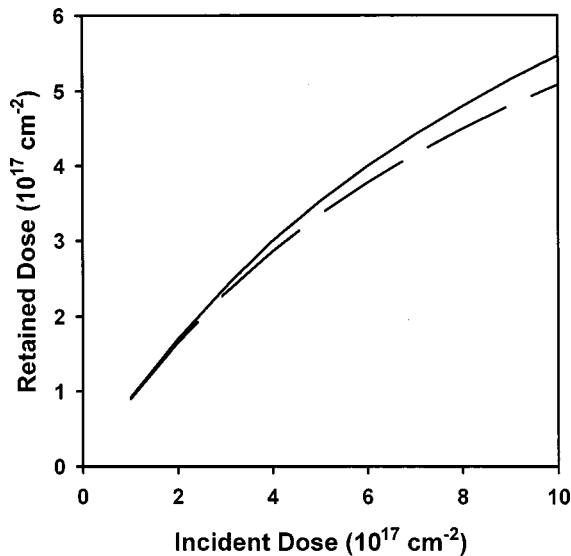


FIG. 4. Retained dose as a function of incident dose for the combined simulation (dashed line) and simulation with identical atomic fluences and incident ion angle distributions, but consisting only of H^+ ions (solid line).

Fig. 3(c). This is, however, a consequence of the high incident dose of H_3^+ , not due to its higher mass. In addition, the lower implantation energy of each H in H_3^+ results in a smaller projected range and sputtering loss is more substantial. Figure 4 exhibits the retained dose as a function of the incident dose for the combined run of all three ion species at the location receiving the highest total incident dose. The curve is seen to roll off at high incident dose. For comparison, we have also simulated the retained dose curve for the same total dose and angular distribution, but for a process made up of entirely H^+ ions, that is, 40 keV per hydrogen atom. The difference between the two curves is not significant. The region close to the edge of the wafer retains a lower percentage of hydrogen, as in these areas, the ions impact at a more oblique angle, but this is somewhat compensated by the higher incident dose near the edge of the wafer. The overall effect is shown in Fig. 3(d).

The maximum incident dose ($1.0 \times 10^{18} \text{ cm}^{-2}$) located at 8.625 cm from the center is 21.5% higher than the minimum incident dose ($8.23 \times 10^{17} \text{ cm}^{-2}$) located at the wafer center. The retained doses at these locations are 5.09×10^{17} and $4.57 \times 10^{17} \text{ cm}^{-2}$, respectively. The difference is only 11.4%, and the maximum difference in the retained dose over the whole wafer is 11.6%. Therefore, the nonuniformity in the retained dose is much less than that in the incident fluence.

Based on our calculation, the surface recession due to sputtering does not exceed 2 nm, except at the very edge of the wafer. The surface recession and average projected range for the combined run along the radial distance is shown in Table I. The projected range is deeper at the center of the wafer (193.5 nm) than at the edge (144.4 nm). This difference is about 34%. However, the projected range is fairly uniform within the radius of 6.375 cm (183.7 nm), the difference being only about 5%. The TAMIX simulated depth profiles for the combined simulation are shown in Fig. 5 for the wafer center, 6.375 cm from the center, and the wafer

TABLE I. Surface recession and average projected range along the radial distance of the wafer. The data are calculated by a combined run of the three species by TAMIX.

Radial distance (cm)	Surface recession (\AA)	Average projected range (\AA)
0.375	8.70	1935
1.125	8.5	1917
1.875	8.1	1931
2.625	7.2	1930
3.375	6.7	1915
4.125	7.6	1905
4.875	8.0	1901
5.625	9.2	1875
6.375	9.6	1837
7.125	12.67	1813
7.875	13.9	1738
8.625	12.6	1691
9.375	16.1	1585
10.125	22.6	1444

edge. The peak becomes shallower toward the wafer edge. The small peak above 400 nm results from H^+ .

IV. CONCLUSION

Hydrogen plasma immersion ion implantation into a 200 mm silicon wafer placed in a plasma consisting of three hydrogen species, H^+ , H_2^+ , and H_3^+ , is simulated by the PIC numerical method. Poisson's equation is modified to take into account the different proportion of the three hydrogen species. The PIC-simulated fluences is subsequently input into TAMIX to calculate the radially dependent retained dose. Four runs are conducted: each species individually and one with all three species together. It is found that the ratio of the retained to incident doses is highest for H^+ , and the ratios for H_2^+ and H_3^+ ions are much lower. This is due to the high fluence of H_3^+ instead of the mass difference. The combined effect of all three species gives rise to a maximum difference in the retained dose of 11.6% along the radial direction, al-

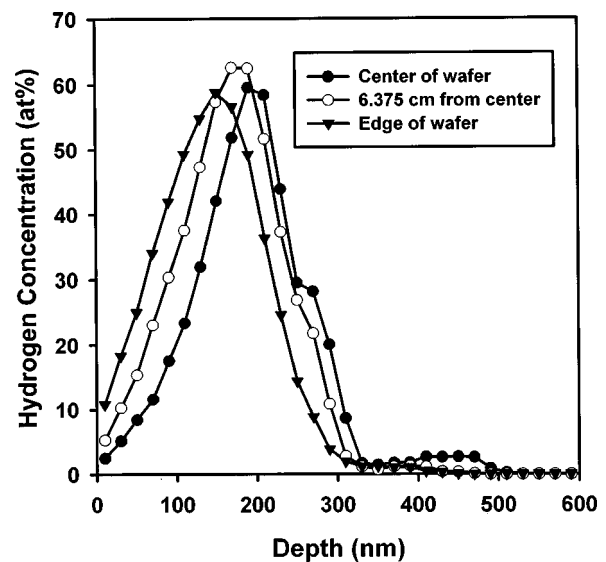


FIG. 5. Implant depth profiles at three different radial locations on the wafer.

though the maximum difference in the incident fluence is 21.5%. This suggests that for this planar geometry, differences in the implantation depth due to off-normal ion incidence can partially compensate for differences in the incident dose due to plasma-sheath dynamics. Differences in the location of the hydrogen peak exist, but within a radius of 6.375 cm, the depth profile is fairly uniform with a variation in the average ion implantation depth of only about 5%. The combined use of PIC that discloses plasma sheath physics and TAMIX that reveals implantation physics present a better picture of reality than either one alone.

ACKNOWLEDGMENT

The work is supported by Hong Kong Research Grants Council Earmarked Grant Nos. 9040332 and 9040344.

- ¹P. K. Chu, S. Qin, C. Chan, N. W. Cheung, and L. A. Larson, *Mater. Sci. Eng.*, **R17**, 207 (1996).
- ²N. W. Cheung, *Mater. Chem. Phys.* **46**, 132 (1996).
- ³P. K. Chu, N. W. Cheung, and C. Chan, *Semicond. Int.* **6**, 165 (1996).
- ⁴J. V. Mantese, I. G. Brown, N. W. Cheung, and G. A. Collins, *MRS Bull.* **21**, 52 (1996).
- ⁵T. Sheng, S. B. Felch, and C. B. Cooper, *J. Vac. Sci. Technol. B* **12**, 969 (1994).
- ⁶B. Mizuno, H. Nakaoka, M. Takase, A. Hori, I. Nakayama, and M. Ogura, in *Extended Abstracts of the 1995 International Conference of Solid State Devices and Materials*, Osaka, Japan, 1995 (unpublished), p. 1041.
- ⁷B. Mizuno, M. Takase, I. Nakayama, and M. Ogura, in *Symposium of VLSI Technology Digest*, Honolulu, 1996 (unpublished), p. 66.
- ⁸S. Qin and C. Chan, *J. Vac. Sci. Technol. B* **12**, 962 (1994).
- ⁹J. Min, P. K. Chu, Y. C. Cheng, J. B. Liu, S. Im, S. Iyer, and N. W. Cheung, *Mater. Chem. Phys.* **40**, 219 (1995).
- ¹⁰J. B. Liu, S. S. K. Iyer, C. M. Hu, N. W. Cheung, R. Gronsky, J. Min, and P. Chu, *Appl. Phys. Lett.* **67**, 2361 (1995).
- ¹¹J. Min, P. K. Chu, Y. C. Cheng, J. Liu, S. S. Iyer, and N. W. Cheung, *Surf. Coat. Technol.* **85**, 60 (1996).
- ¹²P. K. Chu, X. Lu, S. S. K. Iyer, and N. W. Cheung, *Solid State Technol.* **40**, S9 (1997).
- ¹³X. Lu, S. S. K. Iyer, J. B. Liu, C. M. Hu, N. W. Cheung, J. Min, and P. K. Chu, *Appl. Phys. Lett.* **70**, 1748 (1997).
- ¹⁴S. S. K. Iyer, X. Lu, J. B. Liu, J. Min, Z. Fan, P. Chu, C. M. Hu, and N. W. Cheung, *IEEE Trans. Plasma Sci.* **25**, 1128 (1997).
- ¹⁵X. Lu, N. W. Cheung, M. D. Strathman, P. K. Chu, and B. Doyle, *Appl. Phys. Lett.* **71**, 1804 (1997).
- ¹⁶X. Lu, S. S. K. Iyer, C. M. Hu, N. W. Cheung, J. Min, Z. N. Fan, and P. K. Chu, *Appl. Phys. Lett.* **71**, 2767 (1997).
- ¹⁷P. K. Chu, S. Qin, C. Chan, N. W. Cheung, and P. K. Ko, *IEEE Trans. Plasma Sci.* **26**, 79 (1998).
- ¹⁸J. D. Bernstein, S. Qin, C. Chan, and T. J. King, *IEEE Electron Device Lett.* **16**, 421 (1995).
- ¹⁹J. P. Colinge, *Silicon-on-Insulator Technology: Materials to VLSI* (Kluwer, Boston, 1991).
- ²⁰M. M. Bruel, *Nucl. Instrum. Methods, Phys. Rev. B* **108**, 313 (1996).
- ²¹M. Bruel, *MRS Bull.* **23**, 35 (1998).
- ²²T. E. Sheridan, *J. Appl. Phys.* **74**, 4903 (1993).
- ²³X. C. Zeng, T. K. Kwok, A. G. Liu, P. K. Chu, B. Y. Tang, and T. E. Sheridan, *Appl. Phys. Lett.* **71**, 1035 (1997).
- ²⁴T. E. Sheridan, T. K. Kwok, and P. K. Chu, *Appl. Phys. Lett.* **72**, 1826 (1998).
- ²⁵X. C. Zeng, T. K. Kwok, A. G. Liu, P. K. Chu, and B. Y. Tang, *J. Appl. Phys.* **83**, 44 (1998).
- ²⁶Dixon T. K. Kwok, Paul K. Chu, and C. Chan, *IEEE Trans. Plasma Sci.* **26**, (1998).
- ²⁷Z. N. Fan, P. K. Chu, C. Chan, and N. W. Cheung, *Appl. Phys. Lett.* **73**, 202 (1998).
- ²⁸Z. Fan, P. K. Chu, N. W. Cheung, and C. Chan, *IEEE Trans. Plasma Sci.* (to be published).
- ²⁹S. H. Han, G. L. Kulcinski, and J. R. Conrad, *Nucl. Instrum. Methods, Phys. Res. B* **45**, 701 (1990).